Received: March 4, 2014 Revised: April 27, 2014 Accepted: May 23, 2014

(onlinelibrary.wiley.com) DOI: 10.1111/ner.12221

Stimulation Parameters Define the Effectiveness of Burst Spinal Cord Stimulation in a Rat Model of Neuropathic Pain

Nathan D. Crosby, BS*; Melanie D. Goodman Keiser, PhD†; Jenell R. Smith, BS*; Martha E. Zeeman, MS*; Beth A. Winkelstein, PhD*‡

Introduction: Although burst spinal cord stimulation (SCS) has been reported to reduce neuropathic pain, no study has explicitly investigated how the different parameters that define burst SCS may modulate its efficacy. The effectiveness of burst SCS to reduce neuronal responses to noxious stimuli by altering stimulation parameters was evaluated in a rat model of cervical radiculopathy.

Methods: Neuronal firing was recorded in the spinal dorsal horn before and after burst SCS on day 7 following painful cervical nerve root compression ($N = 8$ rats). The parameters defining the stimulation (number of pulses per burst, pulse frequency, pulse width, burst frequency, amplitude) were individually varied in separate stimulation trials while holding the remaining parameters constant. The percent reduction of firing of wide-dynamic-range (WDR) and high-threshold neurons after SCS and the percentage of neurons responding to SCS were quantified for each parameter and correlated to the charge per burst delivered during stimulation.

Results: Pulse number, pulse width, and amplitude each were significantly correlated ($p < 0.009$) to suppression of neuronal firing after SCS. Pulse frequency and amplitude significantly affected ($p < 0.05$) the percentage of responsive neurons. Charge per burst was correlated to a reduction of WDR neuronal firing ($p < 0.03$) and had a nonlinear effect on the percentage of neurons responding to burst SCS.

Conclusions: Burst SCS can be optimized by adjusting relevant stimulation parameters to modulate the charge delivered to the spinal cord during stimulation. The efficacy of burst SCS is dependent on the charge per burst.

Keywords: burst stimulation, neuropathic pain, optimization, radiculopathy, spinal cord stimulation

Conflicts of Interest: Dr. Goodman Keiser is an employee of St. Jude Medical. Dr. Winkelstein has received research funding from St. Jude Medical.

INTRODUCTION

Spinal cord stimulation (SCS) is used to treat a wide range of chronic neuropathic pain conditions by administering electrical stimulation to the dorsal columns of the spinal cord. Traditional SCS uses a tonic paradigm to deliver continuous pulses of various frequencies, pulse widths, and intensities to the spinal cord and is commonly used to manage cervical and lumbar axial and radicular pain (1–3). These parameters can be modulated, along with electrode configuration and placement on the spinal cord, to maximize pain relief for individual patients (4,5). However, tonic stimulation induces paresthesia in the stimulated dermatomes. Although paresthesia can be used to guide electrode placement and programming, many patients prefer paresthesia-free stimulation (4).

Burst SCS is an alternative mode of stimulation that uses small bursts of pulses of stimulation rather than continuous pulses and has been recently reported to reduce neuropathic pain better than tonic SCS without generating paresthesia in the majority of patients (4,6,7). De Ridder et al. (7) found that burst SCS decreased visual analog scale (VAS) pain scores more than tonic SCS for back pain and general pain perception in patients, including those with cervical radicular pain, undergoing brief trials with each stimulation modality. Patients have also reported greater pain relief from burst SCS relative to tonic SCS in a placebo-controlled trial and also when burst SCS was introduced after at least 6 months of tonic stimulation (4,6). Furthermore, burst SCS has been shown to be more effective than tonic SCS for attenuating visceral nociception in a rat model of colorectal distension (8). Although it has been postulated that burst SCS may improve pain suppression over tonic SCS because burst stimulation delivers more charge per second (7), the role of charge delivery in burst SCS has not been investigated.

Burst SCS is highly adaptable by modification of any of the parameters that control the shape of the stimulation waveform—the

Address correspondence to: Beth A. Winkelstein, Department of Bioengineering, University of Pennsylvania, 240 Skirkanich Hall, 210 S. 33rd St, Philadelphia, PA 19104-6321, USA. E-mail: winkelst@seas.upenn.edu

* Department of Bioengineering, University of Pennsylvania, Philadelphia, PA, USA;
† St. Jude Medical, Plano, TX, USA; and
‡ Department of Neurosurgery, University of Pennsylvania, Philadelphia, PA, USA

For more information on author guidelines, an explanation of our peer review process, and conflict of interest informed consent policies, please go to http://www.wiley.com/bw/submit.asp?ref=1094-7159&site=1

Source of funding: This work was supported by a sponsored research contract from St. Jude Medical, as well as fellowship support from the Ashton Foundation.

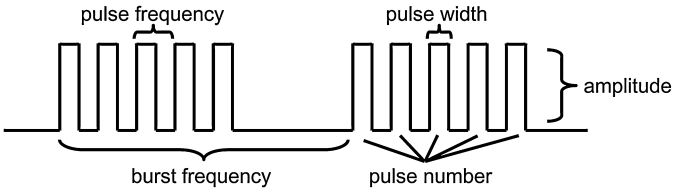

Figure 1. Schematic of a burst spinal cord stimulation waveform indicating the parameters that define the shape of the stimulation: pulse number, pulse frequency, pulse width, burst frequency, and amplitude.

Table 1. Burst Spinal Cord Stimulation Conditions and Parameter Values.

Numbers of pulses	Pulse frequencies (Hz)	Pulse widths (μsec)	Burst frequencies (Hz)	Amplitudes (% of motor threshold)
3	250	250	20	30
5	333	500	40	60
7	500	750	60	90
		1000		

number of pulses per burst, the frequency of pulses within each burst, duration of pulses, the frequency of bursting, or the amplitude (Fig. 1). To date, the clinical and preclinical studies using burst SCS each used the same stimulation parameters: five pulses per burst, 500-Hz pulse frequency, 1-msec pulse width, and 40-Hz burst frequency (4,6–8). Even though tonic SCS is frequently optimized for pain management on a patient-by-patient basis by adjusting pulse width, frequency, and amplitude (9), there have been no published clinical or preclinical studies investigating the optimization of burst SCS for neuropathic pain with respect to any of the parameters defining the stimulation waveform or the charge delivery.

This study tested the hypotheses that burst SCS is effective in reducing dorsal horn neuronal firing associated with cervical radicular pain and that altering burst SCS parameters modulates the effect of stimulation on neurons in the spinal dorsal horn. Although cervical radiculopathy and cervical brachialgia are indications for SCS (1,5,7), preclinical studies have not evaluated the stimulation parameters associated with effective burst SCS for those indications. As such, a model of nerve root compression that induces behavioral sensitivity and spinal neuron hyperexcitability in the rat was used (10–12) to evaluate electrophysiological extracellular recordings of dorsal horn neurons immediately before and after burst SCS. Each burst parameter (Fig. 1; Table 1) was varied across a range of several values that were based on the parameters that could be used for clinical application of burst SCS in order to evaluate the sensitivity of burst SCS effectiveness to each parameter. This study also investigated the modulation of charge per burst as a potential mechanism for the sensitivity of burst SCS to changes in the stimulation parameters.

METHODS

Nerve Root Compression Surgery

Male Holzman rats (386–466 g) were housed under USDA- and AAALAC-compliant conditions with free access to food and water. All experimental procedures were approved by the University of Pennsylvania Institutional Animal Care and Use Committee and carried out under the guidelines of the Committee for Research and Ethical Issues of the International Association for the Study of Pain (13).

Compression of the right C7 dorsal nerve root was performed ($N = 8$ rats) with rats under isoflurane inhalation anesthesia (4% for induction, 2–3% for maintenance) using procedures previously described (14–16). Briefly, with the rat in a prone position, the C6 and C7 vertebrae were exposed by making a midline incision from the base of the skull to the T2 vertebra and separating the overlying muscular tissue. A C6–C7 hemilaminectomy and partial facetectomy on the right side exposed the C7 nerve root between the dorsal root ganglion and the spinal cord. A 10-gf microvascular clip (World Precision Instruments, Sarasota, FL, USA) was placed around the nerve root through a small incision in the dura to compress the root for 15 min. After the surgical procedure, incisions were closed using 3-0 polyester sutures and surgical staples. Rats were monitored during recovery in room air before being returned to normal housing conditions.

Assessment of Behavioral Sensitivity

Behavioral sensitivity was assessed by measuring mechanical hyperalgesia in both forepaws of each rat prior to surgery (baseline) and on days 1, 3, 5, and 7 after nerve root compression. Hyperalgesia was assessed separately in the ipsilateral and contralateral forepaws by quantifying the paw withdrawal threshold (PWT) to application of a series of weighted von Frey filaments (1.4, 2, 4, 6, 8, 10, 15, and 26 g) applied to the plantar surface of the paw (12,14,17). Each filament was applied five times before moving on to the next strongest filament. If the rat displayed a positive response (withdrawing, licking, shaking of the paw) to two consecutive filaments, the lower of the two was recorded as the paw withdrawal threshold. Rats not responding to any of the filaments were assigned the maximum PWT of 26 g. On each designated day, testing was repeated in three rounds separated by at least 10 min, and the average threshold from the three rounds was calculated for each paw and each rat. A repeated-measures ANOVA compared PWT between the ipsilateral and contralateral forepaws at each time point.

Electrophysiology Recordings and Burst Spinal Cord Stimulation

After hyperalgesia testing on day 7, extracellular electrophysiological recordings were acquired to measure neuronal firing before and after burst SCS. Rats were anesthetized with sodium pentobarbital (50 mg/kg, i.p.) and given supplementary doses (5–10 mg/kg, i.p.) as needed based on toe pinch, corneal, and palpebral reflexes (18). A bilateral laminectomy and dural resection from C3 to C7 were performed to expose the spinal cord. Rats were then immobilized on a stereotaxic frame using ear bars and a vertebral clamp at T2 to stabilize the cervical spine (David Kopf Instruments, Tujunga, CA, USA). Core temperature was maintained at 35–37°C using a temperature controller with a rectal probe (Physitemp, Clifton, NJ, USA), and the exposed spinal cord was bathed in 37°C mineral oil for the duration of recording to prevent drying.

A monopolar platinum ball electrode was placed over the dorsal columns at the C3 level, and a grounding electrode was attached to the incised skin on the neck. Constant-current burst SCS was applied using an S48 Grass stimulator with a photoelectric stimulus isolation unit (Grass Technologies, Warwick, RI, USA). The motor threshold (MT) for each rat was identified as the stimulation intensity at which small contractions were first observed in the paraspinal musculature or forelimbs. Extracellular potentials were recorded by lowering a carbon fiber electrode (Kation Scientific, Minneapolis, MN, USA) into the C7 spinal dorsal horn on the side ipsilateral to the

compressed nerve root. Signals were amplified with a gain of 10^3 and conditioned using a passband filter between 0.3 and 3 kHz (World Precision Instruments, Sarasota, FL, USA). The signal was processed with a 60 Hz HumBug adaptive filter (Quest Scientific, North Vancouver, BC, Canada), digitally sampled at 25 kHz (Micro1401, CED, Cambridge, UK), monitored with a speaker for audio feedback (A-M Systems, Carlsborg, WA, USA), and recorded using Spike2 software (CED).

Light-brush and noxious-pinch stimulation of the ipsilateral forepaw were used to identify mechanically sensitive neurons and their receptive fields on the paw. To evaluate changes in neuronal activity due to burst SCS, the neuron (or neurons, if multiple waveforms could be differentiated at a single recording site) underwent SCS trials each consisting of the following: 1) at least 10 seconds of recording to establish baseline spontaneous firing rates; 2) 10 sec of light brushing and 10 sec of noxious pinch by forceps in order to classify the neuron as wide-dynamic-range (WDR) or high-threshold (HT) and to establish pre-SCS evoked firing rates; 3) 10 sec of burst SCS (Fig. 1); and then 4) 10 sec of noxious pinch to record post-SCS evoked firing. Neurons were allowed to recover for at least 20 min between each SCS trial.

The burst SCS parameters were varied for each stimulation trial, with at least three values tested for each parameter (Table 1). For each recording site, the first reference stimulation trial applied burst SCS consisting of seven pulses per burst at 500 Hz with a 1000-μsec pulse width, a burst frequency of 40 Hz, and an amplitude of 90% MT. From that reference parameter set, each of the five parameters was varied individually in subsequent stimulation trials, while the remaining four parameters were held constant (Table 1). Each parameter set was applied in random order during the stimulation trial. When modulating pulse frequency, the interburst interval was not long enough for each burst to contain seven pulses with a 1000-μsec width, so bursts of five pulses were applied. Despite the smaller pulse number, all other parameters remained constant, as pulse frequency was varied in order to allow comparison between different pulse frequency values. Each recording site was used for multiple stimulation trials until the waveform signal was lost.

Electrophysiology Data Analysis

Voltage potentials from each recording site were spike-sorted using Spike2 to differentiate waveforms from multiple neurons. Each neuron was classified either as WDR, if firing was evoked by both light brush and noxious pinch, or HT, if firing was only evoked by a noxious pinch. Low-threshold (LT) neurons, responding only to light mechanical stimuli, were not included in this study as they do not respond to noxious pinch, which was used as the test stimulus. Pre- and post-SCS firing were determined by counting the number of spikes evoked by noxious pinch in the 10 s before and the 10 sec immediately following the application of burst SCS. Voltage potentials during 90% of motor threshold were not measured due to large artifacts masking neuronal activity; therefore, measurements of neuronal responses were only performed before and after SCS. Baseline spontaneous activity was subtracted from the spike counts for each pinch to isolate the neuronal response evoked by the noxious pinch.

Several metrics were used to evaluate the effects of burst SCS on dorsal horn neuronal activity. Change in neuronal firing after burst SCS was calculated as the percent change in spikes evoked by noxious pinch after SCS relative to the number evoked by the pinch that was applied before SCS. Neurons having a negative percent change in firing after burst SCS (a reduction in spikes) were considered to be responsive to burst SCS. The percentage of responsive neurons for each set of stimulation parameters was used as a secondary measure of SCS efficacy. A bivariate linear regression tested for correlation between each burst parameter and changes in neuronal firing among responsive neurons only. The effect of each parameter on the percentage of neurons responding to burst SCS was tested using Fisher's exact test.

The charge per burst delivered to the spinal cord was calculated for each parameter set as the integral of the current applied during a single burst. Changes in WDR and HT neuronal firing were averaged at each charge value across all stimulation trials. The correlations between charge per burst and changes in neuronal firing were then tested for WDR and HT neurons separately using bivariate linear regression. Percentages of responsive WDR and HT neurons in each stimulation trial were binned based on charge per burst; bins were chosen to span the full range of charge values, in 10 equal increments of 0.1 μC. All statistical analyses were performed with $\alpha = 0.05$ using JMP9 (SAS, Cary, NC, USA).

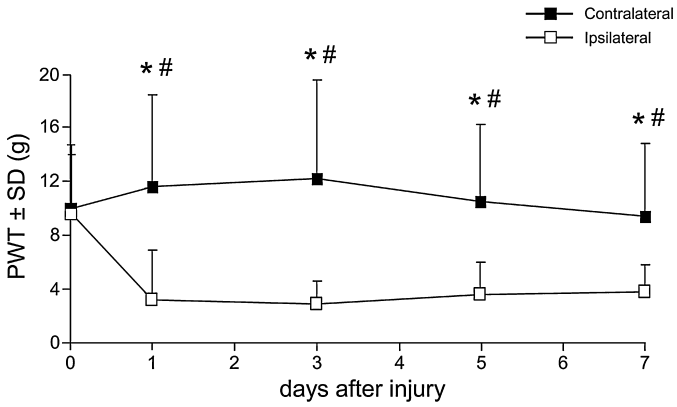

Figure 2. Forepaw paw withdrawal thresholds (PWT) before and after cervical nerve root compression. Nerve root compression induced a significant decrease in PWT for the ipsilateral forepaw compared to both baseline (*p <0.017) and the contralateral forepaw (#p <0.019) on each day after injury.

RESULTS

The PWT of the ipsilateral forepaw was significantly reduced from baseline on each of days 1, 3, 5, and 7 (all p <0.017), and the PWT for the contralateral forepaw was not significantly different from baseline throughout the 7-day period (Fig. 2). In addition, the PWT for the ipsilateral forepaw was significantly lower than the PWT of the contralateral forepaw on all days following nerve root compression (all p <0.019), despite the ipsilateral and contralateral PWTs not being different at baseline (Fig. 2).

Neuronal firing was recorded at 25 different sites in the spinal cord from all rats (3.0 ± 1.1 recording sites per rat). At each recording site, 4.1 ± 1.4 stimulation trials were performed, with 6.8 ± 1.8 separate recording sites tested for each of the five burst SCS parameters investigated in this study. Of the 25 recording sites, nine sites with stable signals were used to test multiple parameters consecutively. Neuronal firing evoked by noxious pinch of the forepaw was attenuated after burst SCS to varying degrees based on the stimulation parameters (Fig. 3). Among the neurons that were responsive to burst SCS (N = 191 neurons from all recording sites and stimulation trials), pulse number (p = 0.0018), pulse width (p = 0.0001), and amplitude (p = 0.0086) each significantly reduced neuronal

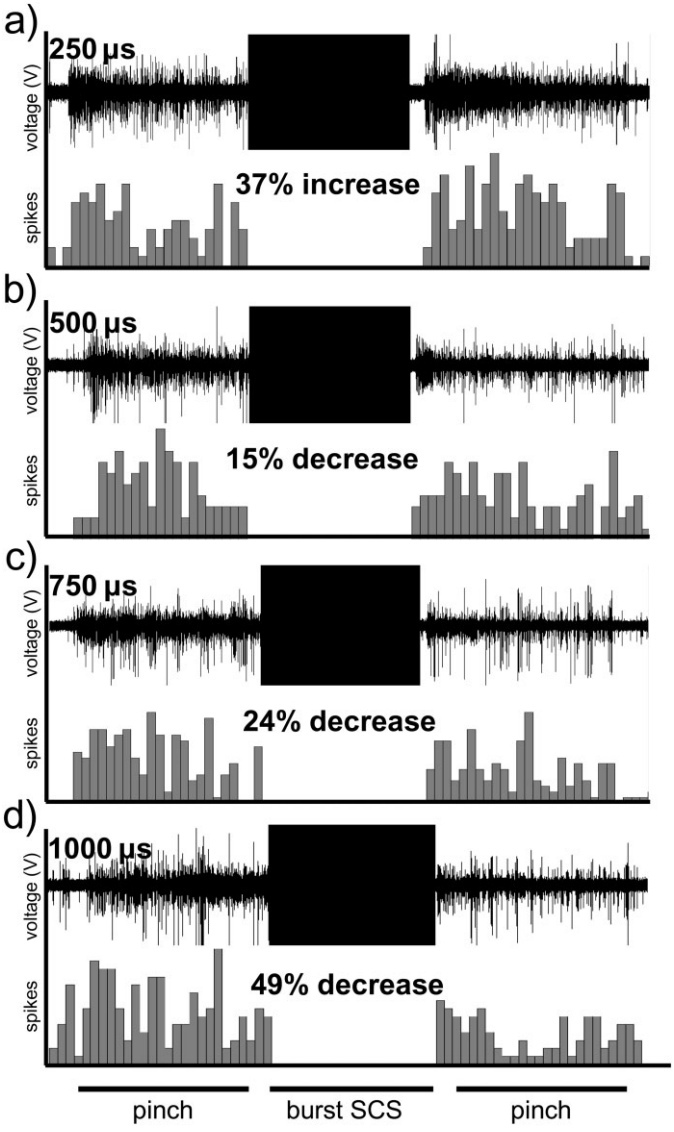

Figure 3. Neuronal firing evoked by a noxious forepaw pinch was attenuated after burst spinal cord stimulation (SCS) to varying degrees depending on the burst parameters. In this representative neuron, activity was suppressed more as pulse width increased from a. 250 µs to b. 500 µs, c. 750 µs, and d. 1000 µs. Here, the other parameters were fixed: pulse number = 7; pulse frequency = 500 Hz; burst frequency = 40 Hz; amplitude = 90% of motor threshold.

responses to noxious stimulation after burst stimulation (Fig. 4). Neuronal firing showed a greater reduction with each increase in these parameters. However, pulse frequency and burst frequency were not correlated to changes in neuronal firing after burst SCS (Fig. 4).

The percentage of responsive neurons exhibiting a reduction in firing after burst SCS was significantly related to the pulse frequency ($p = 0.05$) and the amplitude of stimulation ($p = 0.023$) (Fig. 5). As the pulse frequency and amplitude increased, the percentage of responsive neurons also increased. Although the percentage of responsive neurons also increased with both higher pulse numbers ($p = 0.13$) and pulse widths ($p = 0.078$), those relationships were not significant (Fig. 5). Altering burst frequency had no effect on the percentage of responsive neurons (Fig. 5).

Charge per burst delivered to the spinal cord was highest for the reference parameter set (seven pulses, 500-Hz pulse frequency, 1000-µsec pulse width, 40- Hz burst frequency, 90% MT amplitude), ranging from 0.76–1.07 µC, with some variation due to the differences in MT between rats (Fig. 6a). Pulse number, pulse width, and amplitude were each directly proportional to the charge per burst, so changes in each of those parameters resulted in a wide range of charges per burst during stimulation trials (Fig. 6a). Pulse frequency and burst frequency did not affect charge per burst (Fig. 6a), aside from the variation due to MT differences between rats.

Charge per burst was negatively correlated with changes in neuronal firing among responsive WDR neurons ($N = 141$) after burst SCS ($R^2 = 0.30$, $p = 0.0017$) (Fig. 6b). Among the HT responsive neurons ($N = 50$), neuronal firing also decreased as charge per burst increased, although this correlation was not significant ($R^2 = 0.14$, $p = 0.13$). The total percentage of neurons responding to SCS increased nonlinearly with charge per burst, exhibiting a step transition from 65% responding (35% not responding) at charges below 0.5 µC to 80-85% of neurons responding (15–20% not responding) at charges above 0.5 µC (Fig. 6c). The percentage of WDR neurons responding to burst SCS remained high, averaging 83 ± 6% across all charge values (Fig. 6c). However, the responsiveness of HT neurons exhibited a large increase from 45 ± 4% at charges below 0.5 µC to 78 ± 7% at charges above 0.6 µC; no HT neurons were recorded at parameters having a charge per burst between 0.5 µC and 0.6 µC (Fig. 6c).

DISCUSSION

This study demonstrates that burst SCS reduces neuronal responses to a noxious stimulus in the spinal dorsal horn of rats after a painful compression of the cervical nerve root (Figs. 2–4). Changes in neuronal response following burst SCS are mediated by the stimulation parameters that define the burst waveform. Three parameters in particular—number of pulses per burst, duration of pulses, and amplitude—are each significantly correlated to the changes in neuronal responses after burst SCS (Figs. 4 and 5). Pulse frequency has a significant effect on the percentage of recorded neurons responding to burst SCS (Figs. 4 and 5). Furthermore, the charge per burst delivered to the spinal cord is correlated to the decrease in responses of both WDR and HT neurons after burst SCS (Fig. 6).

The effectiveness of burst SCS, as measured by changes in dorsal horn neuronal firing after stimulation, is dependent on the stimulation parameters. For example, the most effective burst SCS paradigm was found when using the reference parameter settings (seven pulses at 500 Hz and 1000-µsec width, 40-Hz bursts, and 90% MT amplitude), after which neuronal firing was reduced by 44.8 ± 23.3% across the 84.7% of neurons that responded to SCS (Fig. 4c). When the pulse width was adjusted from 1000 µs to 250 µs, neuronal firing was reduced only 15.1 ± 9.4% with 65.4% of neurons responding to stimulation (Fig. 4c). At its maximum effectiveness, burst SCS suppresses up to 44.8% of neuronal activity, which is comparable with the only other study that has applied burst SCS in an animal model of pain (8). That study demonstrated that burst SCS reduced firing in lumbar dorsal horn neurons by 41.5% during noxious colorectal distension (8). Furthermore, the suppression of neuronal firing by burst SCS observed in our study of neuropathic pain is representative of suppression of pain pathways, which may be consistent with reductions in VAS pain scores reported after burst SCS in a clinical study (6). Although burst SCS decreases neuronal activity by suppressing firing in dorsal horn neurons that exhibit hyperexcitability after cervical nerve root compression (10–12), additional studies measuring behavioral sensitivity after

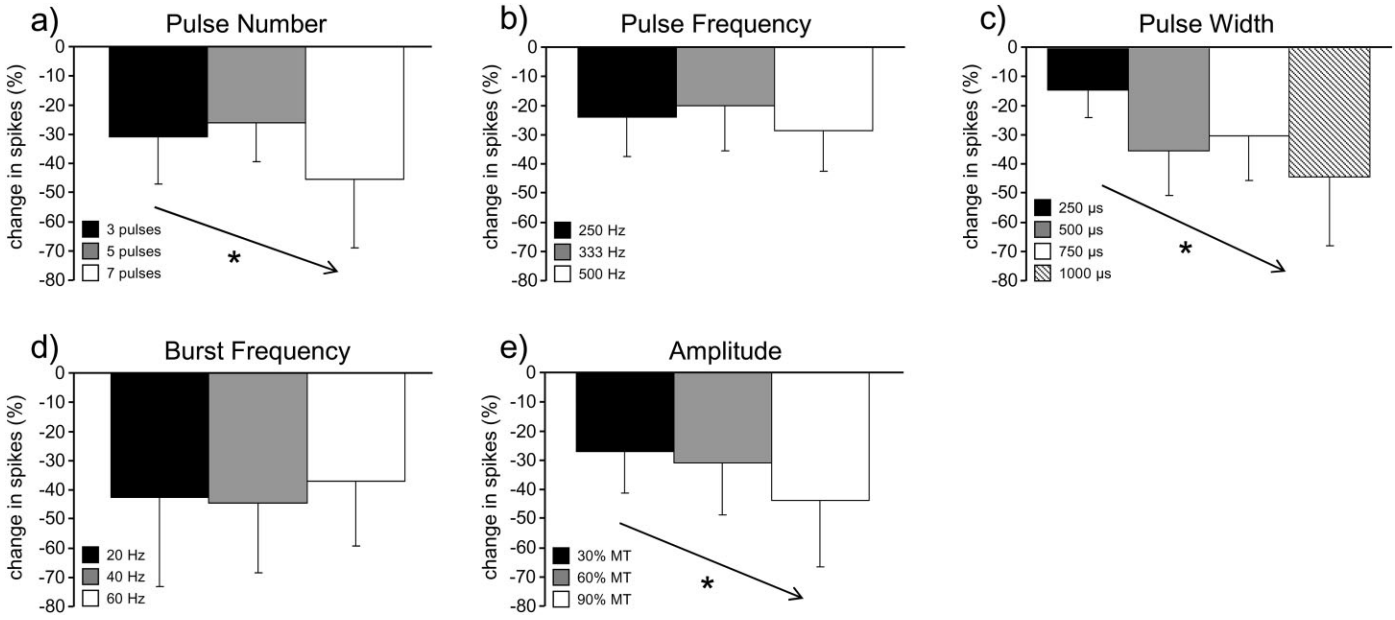

Figure 4. The change in neuronal firing for each set of parameters after burst spinal cord stimulation (SCS) is shown as the percentage change in spikes from before to after burst SCS for each parameter: a. pulse number; b. pulse frequency; c. pulse width; d. burst frequency; and e. amplitude. Asterisks and arrows indicate significant correlations between each of pulse number ($p = 0.0018$), pulse width ($p = 0.0001$), and amplitude ($p = 0.0086$) and a reduction in neuronal activity after burst SCS. MT, motor threshold.

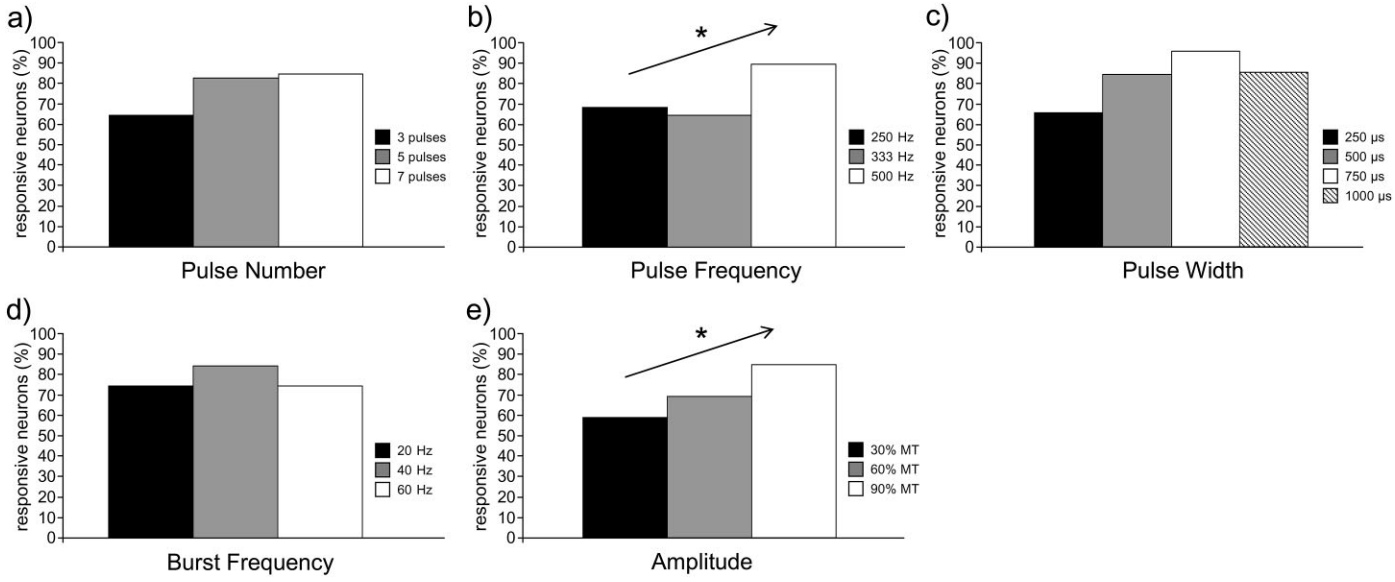

Figure 5. The percentage of responsive neurons responding to burst spinal cord stimulation is shown for each level of the burst parameters: a. pulse number; b. pulse frequency; c. pulse width; d. burst frequency; and e. amplitude. Asterisks and arrows indicate significant positive correlations of each of pulse frequency ($p = 0.05$) and amplitude ($p = 0.023$) to the percentage of responsive neurons. MT, motor threshold.

SCS are needed to draw more direct conclusions about modulation of pain by burst SCS.

The reduction in neuronal response to noxious pinch following burst SCS is significantly correlated to charge per burst delivered during stimulation (Fig. 6b). Antidromic activation of inhibitory interneurons by large-diameter Aβ fibers suppresses firing in dorsal horn neurons to block nociceptive signaling, as proposed by the gate theory of pain and supported by reports of attenuation of dorsal horn excitability by dorsal column stimulation (19–23). Increased current penetration and charge delivery may increase antidromic activation of large-diameter Aβ fibers in the dorsal columns (2,24), resulting in the decreases in WDR and HT neuronal activity that are observed at higher charges (Figs. 3 and 4). The charge per burst is also nonlinearly related to the percentage of neurons responding to burst SCS, most notably an increase in responsive HT neurons at higher charges (Fig. 6c). As charge delivery increases, stimulation may activate fibers of decreasing diameter that have higher activation thresholds (24,25), increasing the number of active dorsal column fibers and overall inhibitory tone in the dorsal horn. The percentage of responsive WDR neurons

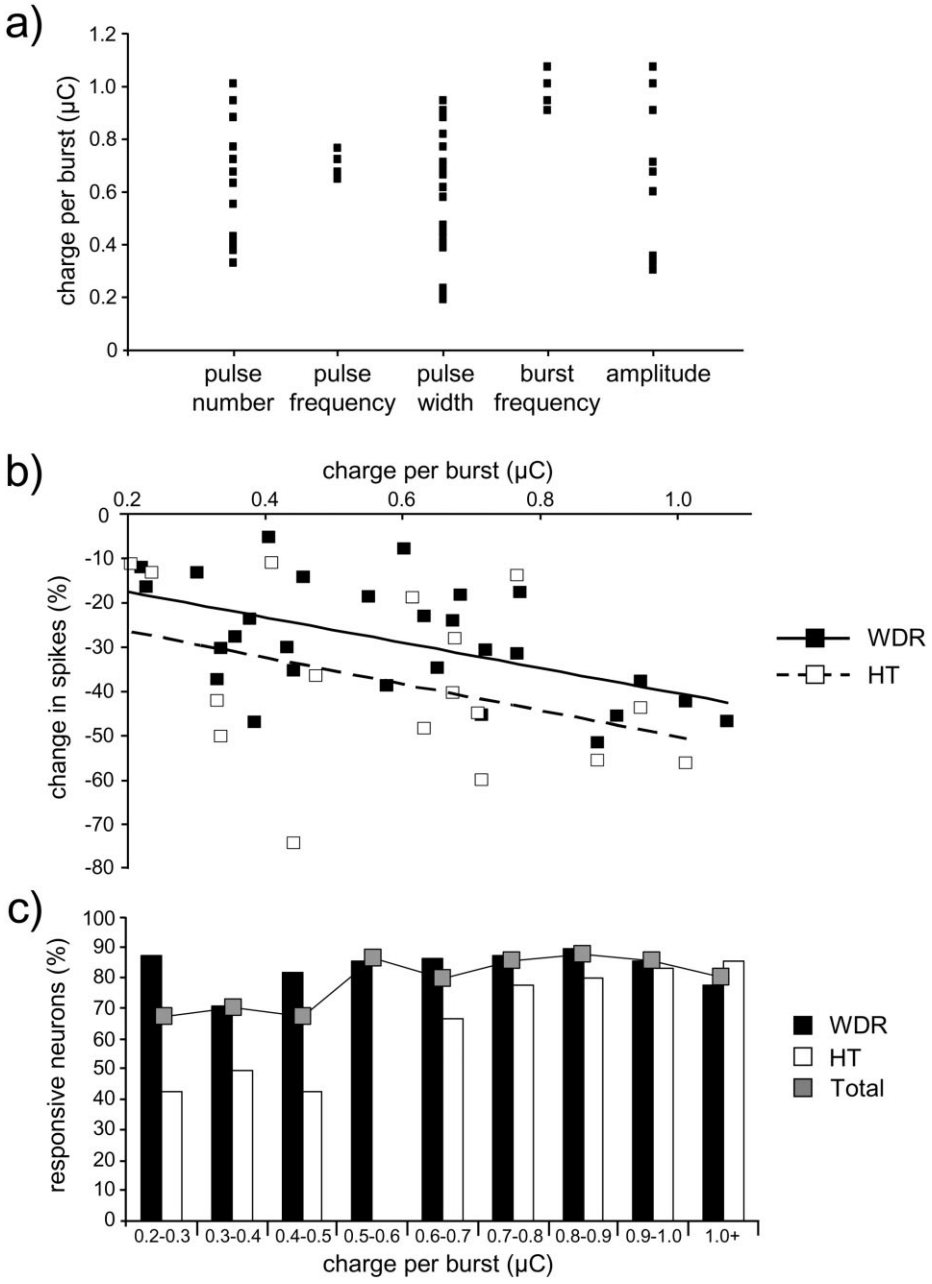

Figure 6. a. Pulse number, pulse width, and amplitude had the greatest range of charges tested across the stimulation trials associated with each parameter. Charge was constant across all pulse frequencies and across all burst frequencies, aside from small variations due to motor threshold differences between rats. b. Percentage change in firing of wide-dynamic-range (WDR) and high-threshold (HT) neurons was correlated to charge per burst, but the correlation was significant only for WDR neurons ($p = 0.0017$). c. The percentage of WDR neurons responding to spinal cord stimulation (SCS) was unchanged by charge per burst; the percentage of HT neurons responding to burst SCS exhibited a step that was also evident in the total percentage of responsive neurons, increasing when charge per burst exceeded 0.5 μC. No HT neurons were collected in the 0.5 to 0.6 μC per burst range.

remained constant and was higher than HT neurons at low charge values (Fig. 6c), suggesting that WDR neurons are more susceptible than HT neurons at low charges to the stimulation-induced attenuation of dorsal horn neuronal firing (21,23). Despite the increase in responsive HT neurons observed at higher charges, a subset of neurons (15–40% of both WDR and HT neurons) never responded to burst SCS in this study (Figs. 4 and 6c) regardless of increasing burst parameters. Computational models of fiber recruitment during dorsal column stimulation suggest that SCS activates fibers that are located near the surface of the dorsal columns (24). It is possible that the unresponsive dorsal horn neurons may be those that are inhibited only by activity in deeper dorsal column fibers that are not recruited by burst SCS in this study. However, additional models of dorsal column fiber activation during SCS suggest that multicontact arrays can offer greater control of stimulation field breadth and depth (26,27) and may activate deeper dorsal column fibers more efficiently to reduce firing in nonresponsive dorsal horn neuron populations.

Among the individual parameters investigated here, pulse number, pulse width, and amplitude each have substantial

influence on the effectiveness of burst SCS, correlating to both reductions in neuronal firing and increases in the percentage of responsive neurons (Figs. 4 and 5). These are also the only parameters with effects that are directly proportional to charge per burst and the greatest range of charges tested across stimulation trials (Fig. 6a), which suggests that modulation of charge per burst regulates the effectiveness of burst SCS. Increases in pulse frequency resulted in a greater percentage of neurons responding to burst SCS, especially at the highest pulse frequency (500 Hz) (Fig. 5b). Afferent fibers are activated in a frequency-specific fashion by sine-wave stimulation, with the large-diameter Aβ fibers found in the dorsal columns progressively activated as stimulation frequencies increase from 5 to 250 to 2000 Hz (6,8,28). Although studies of frequency-dependent neuronal activation have not been performed with the square-wave stimulation used in SCS, increases in burst SCS pulse frequency may selectively activate more Aβ fibers in the dorsal columns and inhibit larger numbers of WDR and HT neurons in the dorsal horn without changing charge per burst. However, higher pulse frequencies do not directly result in a corresponding decrease in neuronal firing; therefore, increased stimulation frequency may also require accompanying changes in other parameters that *do* increase charge per burst in order to enhance suppression of neuronal firing. Potential interaction effects from modulating two or more stimulation parameters could alter the effectiveness of burst SCS in a manner not predicted by the results of this study, in which parameters were evaluated separately while controlling for interactions with the other parameters. However, the correlation between charge per burst and the effectiveness of stimulation (Fig. 6) suggests that the overall effect of modulating multiple parameters depends on the change in charge delivery; nevertheless, studies are needed to evaluate specific interactions between parameters.

This study investigated the parameters that collectively define the shape and intensity of burst stimulation, but other elements of SCS can be modified to adjust charge delivery. For example, monopolar electrodes deliver higher charge densities than bipolar and tripolar stimulation, suggesting that electrode configuration plays an important role in determining charge densities at the surface of the spinal cord (29). Electrodes with small surface areas also yield higher charge densities by concentrating current delivery on a smaller contact area (29). This study used a monopolar ball-shaped electrode, which, although commonly used in preclinical studies (8,23), may deliver current differently from the directed stimulation that is applied by the insulated bipolar electrode arrays that are used clinically. Because electrode geometry and polarity (monopolar, bipolar, or multipolar) can differentially affect the activation of dorsal column fibers (30,31), studies are needed to characterize burst stimulation parameters in larger multielectrode arrangements with cathode and anode arrangements that simulate those used clinically. It is also important to note that as with any animal model, additional studies are needed to fully evaluate the optimization and relative effectiveness of burst SCS in the human. While animal models enable focused evaluation of specific mechanisms, findings do not always translate to the human, owing in part to the difference in lifetimes between the species.

This study showed that burst SCS is effective for reducing neuronal responses to noxious stimulation in the dorsal horn after painful root compression, but the high variability in published clinical outcomes suggests that understanding of burst stimulation parameters is needed to effectively manage pain. Charge per burst is significantly correlated to the effectiveness of burst SCS, indicating that changing the parameters to increase the amount of charge delivered to the spinal cord may in turn increase pain relief in patients. Overall, this study suggests that patient-specific optimization of burst SCS by modulating its stimulation characteristics may provide a greater therapeutic range for SCS.

Authorship Statement

Mr. Crosby and Drs. Goodman Keiser and Winkelstein designed the study, including data collection and data analysis. The manuscript was drafted by Mr. Crosby, with revision and intellectual contribution by Drs. Winkelstein and Goodman Keiser. N. Crosby, J. Smith, and M. Zeeman performed animal surgeries and monitoring.

How to Cite This Article

Crosby N.D., Goodman Keiser M.D., Smith J.R., Zeeman M.E., Winkelstein B.A. 2015. Stimulation Parameters Define the Effectiveness of Burst Spinal Cord Stimulation in a Rat Model of Neuropathic Pain. Neuromodulation 2015; 18: 1–8

REFERENCES

1. Alo KM, Redko V, Charnov J. Four year follow-up of dual electrode spinal cord stimulation for chronic pain. *Neuromodulation* 2002;5:79–88.
2. Compton AK, Shah B, Hayek SM. Spinal cord stimulation: a review. *Curr Pain Headache Rep* 2012;16:35–42.
3. Stojanovic MP, Abdi S. Spinal cord stimulation. *Pain Physician* 2002;5:156–166.
4. De Vos CC, Bom MJ, Vanneste S, Lenders MWPM, de Ridder D. Burst spinal cord stimulation evaluated in patients with failed back surgery syndrome and painful diabetic neuropathy. *Neuromodulation* 2014;17:152–159.
5. Rizvi S, Kumar K. A case for spinal cord stimulation therapy—don't delay. *Pract Pain Manag* 2013;13:48–61.
6. De Ridder D, Plazier M, Kamerling N, Menovsky T, Vanneste S. Burst spinal cord stimulation for limb and back pain. *World Neurosurg* 2013;80:642–649.
7. De Ridder D, Vanneste S, Plazier M, van der Loo E, Menovsky T. Burst spinal cord stimulation: toward paresthesia-free pain suppression. *Neurosurgery* 2010;66: 986–990.
8. Tang R, Martinez M, Goodman-Keiser M, Farber JP, Qin C, Foreman RD. Comparison of burst and tonic spinal cord stimulation on spinal neural processing in an animal model. *Neuromodulation* 2014;17:143–151.
9. Smits H, van Kleef M, Holsheimer J, Joosten EAJ. Experimental spinal cord stimulation and neuropathic pain: mechanisms of action, technical aspects, and effectiveness. *Pain Pract* 2013;13:154–168.
10. Nicholson KJ, Gilliland TM, Winkelstein BA. Upregulation of GLT-1 by treatment with ceftriaxone alleviates radicular pain by reducing spinal astrocyte activation and neuronal hyperexcitability. *J Neurosci Res* 2014;92:116–129.
11. Smith JR, Syré PP, Oake S et al. Salmon and human thrombin differentially regulate radicular pain, glial-induced inflammation and spinal neuronal excitability through the protease-activated receptor-1. *PLoS ONE* 2013;8:e80006.
12. Zhang S, Nicholson KJ, Smith JR, Syré PP, Gilliland TM, Winkelstein BA. The roles of mechanical compression and chemical irritation in regulating spinal neuronal signaling in painful cervical nerve root injury. *Stapp Car Crash J* 2013;57:219–242.
13. Zimmerman M. Ethical guidelines for investigations of experimental pain in conscious animals. *Pain* 1983;16:109–110.
14. Hubbard RD, Winkelstein BA. Transient cervical nerve root compression in the rat induces bilateral forepaw allodynia and spinal glial activation: mechanical factors in painful neck injuries. *Spine* 2005;30:1924–1932.
15. Rothman SM, Winkelstein BA. Chemical and mechanical nerve root insults induce differential behavioral sensitivity and glial activation that are enhanced in combination. *Brain Res* 2007;1181:30–43.
16. Rothman SM, Winkelstein BA. Cytokine antagonism reduces pain and modulates spinal astrocytic reactivity after cervical nerve root compression. *Ann Biomed Eng* 2010;38:2563–2576.
17. Chang YW, Winkelstein BA. Schwann cell proliferation and macrophage infiltration are evident at day 14 after painful cervical nerve root compression in the rat. *J Neurotrauma* 2011;28:2429–2438.
18. Field KJ, White WJ, Lang CM. Anaesthetic effects of chloral hydrate, pentobarbitone and urethane in adult male rats. *Lab Anim* 1993;27:258–269.
19. Daniele CA, MacDermott AB. Low-threshold primary afferent drive onto GABAergic interneurons in the superficial dorsal horn of the mouse. *J Neurosci* 2009;29: 686–695.
20. Dubuisson D. Effect of dorsal-column stimulation on gelatinosa and marginal neurons of cat spinal cord. *J Neurosurg* 1989;70:257–265.

21. Guan Y, Wacnik PW, Yang F et al. Spinal cord stimulation-induced analgesia: electrical stimulation of dorsal column and dorsal roots attenuates dorsal horn neuronal excitability in neuropathic rats. *Anesthesiology* 2010;113:1392–1405.
22. Melzack R, Wall PD. Pain mechanisms: a new theory. *Science* 1965;150:971–979.
23. Yakhnitsa V, Linderoth B, Meyerson BA. Spinal cord stimulation attenuates dorsal horn neuronal hyperexcitability in a rat model of mononeuropathy. *Pain* 1999;79:223–233.
24. Holsheimer J. Which neuronal elements are activated directly by spinal cord stimulation. *Neuromodulation* 2002;5:25–31.
25. Kreis PG, Fishman SM. *Spinal cord stimulation: percutaneous implantation techniques*. New York: Oxford University Press, 2009.
26. Manola L, Holsheimer J, Veltnik PH, Bradley K, Peterson D. Theoretical investigation into longitudinal cathodal field steering in spinal cord stimulation. *Neuromodulation* 2007;10:120–132.
27. Sankarasubramanian V, Buitenweg JR, Holsheimer J, Veltnik P. Triple leads programmed to perform as longitudinal guarded cathodes in spinal cord stimulation: a modeling study. *Neuromodulation* 2011;14:401–411.
28. Koga K, Furue H, Rashid MH, Takaki A, Katafuchi T, Yoshimura M. Selective activation of primary afferent fibers evaluated by sine-wave electrical stimulation. *Mol Pain* 2005;1:13–23.
29. Wesselink WA, Boom HBK. Analysis of current density and related parameters in spinal cord stimulation. *IEEE Trans Rehabil Eng* 1998;6:200–207.
30. Holsheimer J, Struijk JJ. How do geometry factors influence epidural spinal cord stimulation: a quantitative analysis by computer modeling. *Stereotact Funct Neurosurg* 1991;56:234–249.
31. Holsheimer J, Struijk JJ, Tas NR. Effects of electrode geometry and combination on nerve fibre selectivity in spinal cord stimulation. *Med Biol Eng Comput* 1995;33:676–682.

COMMENT

This is an important study, well designed and well performed. It fulfills the strong need for more basic knowledge about underlying mechanisms in efficacy of spinal cord stimulation.

Frank Huygen, MD, PhD
Rotterdam, The Netherlands

Comments not included in the Early View version of this paper.

